Indian Journal of Engineering & Materials Sciences
Vol. 32, December 2025, pp.765-772
DOI:10.56042/ijems,v32i06.23858

Molecular SETs with enhanced electrostatic control: A tri-gated architecture using vanadium tris(dithiolene) as a quantum island

Anu[a], Priti Goyal[b*], Manisha Verma[b], Mohd. Shahid Khan[a], Anurag Srivastava[c], Sunita Hooda[d] & Sanjeeta Rani[b*]

[a]Department of Physics, Jamia Millia Islamia, New Delhi 110 025, India

[b]Department of Physics, Acharya Narendra Dev College, University of Delhi, New Delhi 110 019, India

[c]Advanced Material Research Group, CNT Lab, ABV-Indian Institute of Information Technology and Management, Gwalior 474 015, India

[d]Department of Chemistry, Acharya Narendra Dev College, University of Delhi, New Delhi 110 019, India

Received:16 September 2025 ; accepted:05 December 2025

Single-electron transistors (SETs) have emerged as promising candidates for low-power nanoelectronic applications due to their ability to control electron flow at the single-charge level. However, conventional SETs have faced challenges such as limited charge-state tunability, cross-talk, and reduced electrostatic precision as device dimensions have scaled down. To address these limitations, this study has presented a theoretical investigation of a tri-gate single-electron transistor (TG-SET) that has incorporated a redox-active vanadium tris(dithiolene) complex, $V(edt)_3$, as the molecular island. The TG-SET architecture has introduced three independently controlled gate electrodes positioned around the molecular channel to enable spatially resolved electrostatic modulation. Using density functional theory (DFT) and non-equilibrium Green's function (NEGF) calculations, the study has modeled the electronic structure and transport behaviour under varying gate voltages and charge states. The results have revealed stable Coulomb blockade plateaus, spin-resolved energy levels, and nonlinear current–voltage characteristics, demonstrating fine-tuned control over molecular charge and orbital alignment. A key outcome has included the extraction of gate–molecule coupling parameters through total energy fitting across multiple charge configurations. The TG-SET has exhibited enhanced gate sensitivity, reduced leakage potential, and improved charge selectivity compared to conventional SETs. This work has highlighted the potential of tri-gated architectures in advancing molecular-scale electronics and has provided a design framework for future experimental realization. The findings have opened new directions for the development of multifunctional, ultra-low-power devices in quantum computing, sensing, and molecular logic applications.

Keywords: Charge stability, Density functional theory, Electrostatic control, Non-equilibrium Green's function, Single-electron transistor, Tri-gated (TG) SET

1 Introduction

Single-electron transistors (SETs) are nanoscale switching devices that rely on the controlled movement of individual electrons, allowing for extremely energy-efficient operation. As these devices scale down, their performance improves, making them ideal candidates for next-generation nanoelectronic circuits. Beyond their switching capabilities, SETs serve as valuable platforms for probing electron addition energies and investigating energy-level distributions in quantum dots and molecular systems[1,2]. Their quantized transport behaviour allows for highly precise charge detection, which is vital in applications like single-electron boxes and ultrasensitive detectors[3,4]. SETs have also demonstrated potential in infrared detection at room temperature and in functioning as microwave detectors, further expanding their application scope. Additionally, their compatibility with conventional CMOS technologies facilitates their integration into hybrid nanoelectronic systems, where power efficiency and miniaturization are essential.

In the past, a wide range of SET architectures has been explored using both inorganic and organic materials, each offering distinct advantages and challenges. Molecules such as benzene, anthracene, and boron-functionalized anthracene (10-boranylanthracene-9-yl) have been studied within SET frameworks for their electroactive behaviour and chemical stability[5,6]. Applications have extended to molecular-scale sensing, with studies reporting nicotine detection using single-molecule transistors (SMTs)[7]. Further investigations have focused on

Corresponding authors
(E-mail: sanjeetarani@andc.du.ac.in , pritigoyal@andc.du.ac.in)

polarization effects in organic systems like OPV5[8] and room-temperature SET operation using scanning tunneling microscopy (STM) on titanium-based materials[9]. Foundational work in the field has deepened our understanding of single-electron charging in small tunnel junctions[10], while additional studies have introduced advanced materials, including metal-organic frameworks based on thiophene and benzothiophene, to improve stability and conductance in SETs[11,12]. In the last few years, metal-organic complexes have attracted particular interest for their unique redox properties and structural versatility. Several studies have shown that incorporating these compounds as SET islands can enhance charge transport behaviour and long-term device stability[13–16]. Among these, thiophene-based systems have received growing attention due to their π-conjugation, mechanical robustness, and favorable electronic characteristics[17].

Despite these advances, most previous SET designs have relied on single-gate (SG) or double-gate (DG) architectures[18], both of which inherently limit the control that can be exerted over the charge and spin states of the molecular island. SG-SETs offer only coarse modulation, while DG-SETs, though an improvement, often suffer from gate cross-talk and increased leakage currents as devices scale down. These architectural limitations point to a critical research gap: the need for SETs that can offer precise, multidimensional electrostatic control to enable fine-tuning of molecular charge and spin states at low power.

This study directly addresses this gap by introducing a tri-gate single-electron transistor (TG-SET) based on the redox-active, spin-capable organometallic molecule vanadium tris(dithiolene), $V(edt)_3$, providing a substantial leap forward in molecular electronics. By integrating a triple-gate architecture with a chemically tunable and electronically robust molecule, this TG-SET enables sub-millivolt resolution in electrostatic modulation and unlocks a new regime of controllable charge, spin, and orbital dynamics at the molecular level. The result is a device that overcomes key limitations of SG and DG SETs by minimizing gate interference, enhancing orbital alignment, and improving tunneling efficiency, features essential for multifunctional, low-power nanoelectronic and sensitive charge detection applications[19].

The $V(edt)_3$ complex was chosen for this study due to its exceptional electrochemical properties and structural stability. This molecule, derived from thiophene ligands and a vanadium center, exhibits reversible redox activity between V(IV) and V(VI), supporting stable charge states that correspond to distinct Coulomb blockade plateaus. Its narrow and tunable HOMO–LUMO energy gap facilitates efficient electron transport at low gate voltages, while its planar and symmetric geometry ensures persistent electrode coupling across charge transitions. The π-conjugated dithiolene ligands distribute charge density effectively across the molecule, enabling resonance tunneling and enhancing conductance when energy levels align with the Fermi levels of the electrodes. Additionally, the molecular framework of $V(edt)_3$can be chemically modified to fine-tune redox potentials and orbital energy levels, allowing for tailored electronic behaviour suited to specific device needs. The relatively compact and symmetric structure of $V(edt)_3$ makes it highly amenable to theoretical modeling using density functional theory (DFT) and non-equilibrium Green's function (NEGF) techniques. These simulations offer predictive insights into charge transport behaviour, energy-level alignment, and current–voltage characteristics under various gating conditions. Integrating the $V(edt)_3$ complex into a triple-gate architecture brings a new dimension of control to SET design. Unlike SG or DG configurations, the TG-SET allows independent voltage control over three spatially distinct regions around the molecule. This enables highly localized field modulation, reduces short-channel effects, and improves gate efficiency. Such fine control is particularly important in pushing SETs toward applications in quantum logic, molecular memory, and charge-sensitive biosensors.

Simulations performed in this work—using DFT coupled with NEGF methods—confirm the expected advantages of the TG-SET architecture. The system exhibits nonlinear transport characteristics, clear Coulomb blockade features, and multiple resonant tunneling events. These findings underscore the potential of this platform to support advanced functionalities such as multilevel logic, non-volatile memory, and quantum-dot-like charge retention.

Thus, this study fills a crucial gap in molecular SET research by presenting the first comprehensive modeling of a tri-gate architecture combined with a redox-active, tunable vanadium complex. By offering improved control, higher sensitivity, and lower power operation, the TG-SET design introduced here lays

the groundwork for the next generation of molecular-scale electronics. With applications ranging from quantum information processing to biomedical sensing, this approach could enable a new class of ultra-efficient, multifunctional nanoelectronic devices.

2 Materials and Methods

In this section we describe the TG-SET architecture introducing three independently controlled gate electrodes positioned around the molecular channel to enable spatially resolved electrostatic modulation. To examine the performance of the TG-SET, preliminary calculations were conducted using Density Functional Theory (DFT) and the Non-Equilibrium Green's Function (NEGF) approach.

2.1 Device structure and modeling

A Single-Electron Transistor (SET) features a central island that's flanked by the electrodes viz. source, drain, and gate. To minimize gate leakage and avoid any distortion of the molecular signature, between the gate and island, a dielectric layer is added. A single electron's travel is mostly controlled by the gate electrode, which makes it simpler for it to get to the island from the source and subsequently to the drain. via quantum mechanical tunneling. The operation of SET is governed by the Coulomb blockade regime, which happens as a result of the island and electrodes' poor coupling. In this condition, for an electron to go from the source to the drain via the island, its energy level must fall within the applied bias window. During this process, for a limited time, the electron stays confined on the island, leading to quantum state decoherence. Consequently, the electron tunneling from the source to the island is no longer essential for the tunneling process from the island to the drain. Figures 1(a−c) illustrates the schematics of SG, DG, and TG SETs, respectively.

To examine the performance of the TG-SET, preliminary calculations were conducted using density functional theory (DFT) and the non-equilibrium Green's function (NEGF) approach. The energy calculations revealed a significant enhancement in electrostatic control with the introduction of a third gate, leading to improved charge modulation. The computed total energies were used to determine key parameters such as ionization energy, affinity energy, and addition energy, all of which exhibited lower values in the TG-SET compared to conventional SET designs. These energy values were further employed to generate charge stability diagrams and energy surface plots across

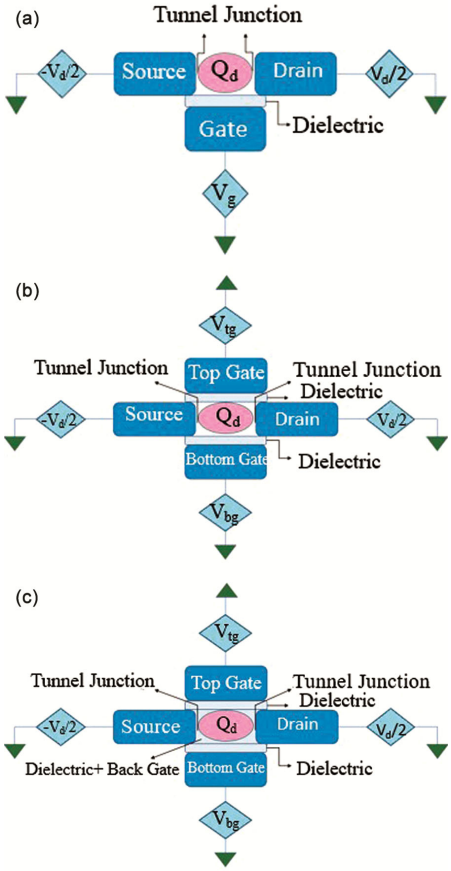

Fig.1 — Schematic diagram of single electron transistor (SET) (a) With a conventional single-gate control mechanism, (b) Double gated with both top and bottom gates and (c) Tri gated, which further enhances charge modulation and minimizes leakage currents.

various gate voltages, confirming improved conduction characteristics. Furthermore, due to its high sensitivity to individual charge states, the TG-SET demonstrates strong potential for applications as an ultra-sensitive charge sensor, making it highly suitable for nanoelectronic and quantum computing applications.

2.2 Computational details

Computational modeling of the V(edt)$_3$ molecule and its integration into single, double, and triple-gated single-electron transistors (SETs) was carried out using Gaussian 03 software with the B3LYP method and the LANL2DZ basis set[20]. The structural configurations of these SETs are illustrated in Figs 2(a−d).

Each SET configuration is enclosed in a simulation box with dimensions (19.34 × 15.27 × 19.91) Å. Within this box:

- A gate electrode of 1 Å thickness is positioned in the xz plane.

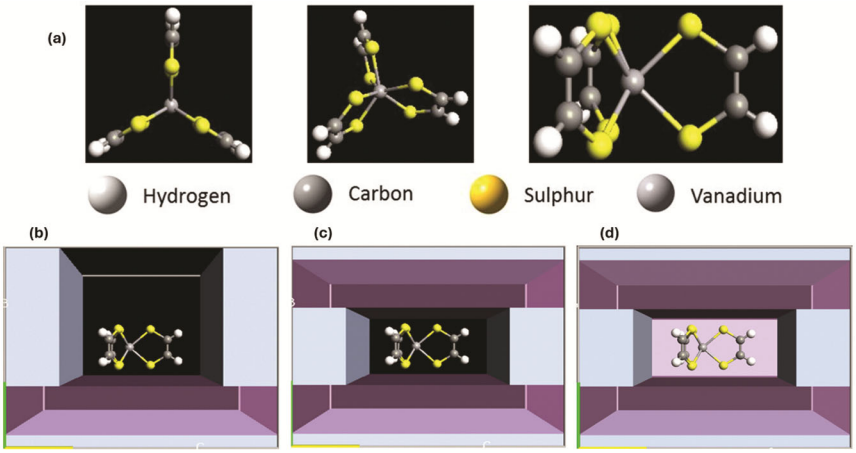

Fig. 2 — Structural configurations of (a) Optimized V(edt)$_3$ molecule, (b) Modeled single gate SET, (c) Modeled double gate SET and (d) Modeled tri gate SET.

- A gate dielectric with a relative permittivity of $10\epsilon_0$ and a thickness of 3.7 Å is placed above the gate.
- The electrodes of source and drain, each ~4 Å thick in the xy plane, encircle the island molecule, which is centered above the dielectric.
- The separation between the three electrodes is fixed at 2.8 Å, functioning as a capacitive tunnel junction, where electron tunneling occurs.

To maintain numerical stability, the SET model operates under Neumann boundary conditions, ensuring that no perpendicular electric field components are present at the boundaries. Information on the calculating process is available in the literature[21,22]. For multi-gate configurations, additional gate electrodes (with the same specifications) can be incorporated into the single-gate setup, progressively transforming it into double-gate, triple-gate, and four-gate configurations. These modifications significantly enhance electrostatic control over the island region. However, this study focuses exclusively on the TG-SET, which exhibits superior electrostatic control and charge modulation. The work function for the electrodes was set at 5.28 eV, consistent with gold, ensuring an accurate representation of charge transport behaviour[23].

We used the Atomistic Toolkit (ATK) Virtual NanoLab (VNL) simulation program to carry out ab initio calculations utilizing the density functional theory (DFT) based methodology in order to determine the charging energy by implementing local density approximations (LDA), while incorporating exchange–correlation effects and a double-zeta polarized basis set for enhanced accuracy[24, 25].

These computational techniques ensure precise modeling of electronic properties and provide reliable energy estimations for the TG-SET.

3 Results and Discussion

Figure 2(a) shows the optimized molecule using literature structural values[26]. We modeled the single, double, and TG-SETs using the optimized molecule in accordance with the guidelines provided in section 2.2, and shown in Figs 2(b−d) earlier.

After completing the modeling, we examined the conduction characteristics of the TG-SET by analyzing their energies under various conditions. We determined the total energy (E_{total}) for various charge states q at different voltages of the gate at the bottom ($V_{bg} = -8.0, -6.0, -4.0, -2.0, 0, 2.0, 4.0, 6.0, 8.0, 10.0, 12.0\ V$) to investigate the basic connection between V_{bg} and E_{total} (Fig. 3(a-d)). The molecule having q = 0 in the SG SET has the lowest energy at $V_{bg} = 0\ V$, which is found to be shifted to $V_{bg} = 12\ V$ for TG-SET.

Ionization energy (the energy that is released or absorbed when a molecule loses an electron) and affinity energies (the energy that is captured or released when a molecule gains an electron), have been determined using E_{total} , as shown in Table 1.

It can be seen from the table that almost all these values are found to decrease for the TG-SET, and the addition energy—the difference between the first ionization and first affinity—also lowers for the TG-SET, thereby enhancing its conductivity compared to the single & double-gated SET. Additionally, it has been observed that the V(edt)$_3$ molecule has lower ionization values than SETs based on organic and inorganic islands[27,28], suggesting that it is a superior promising island.

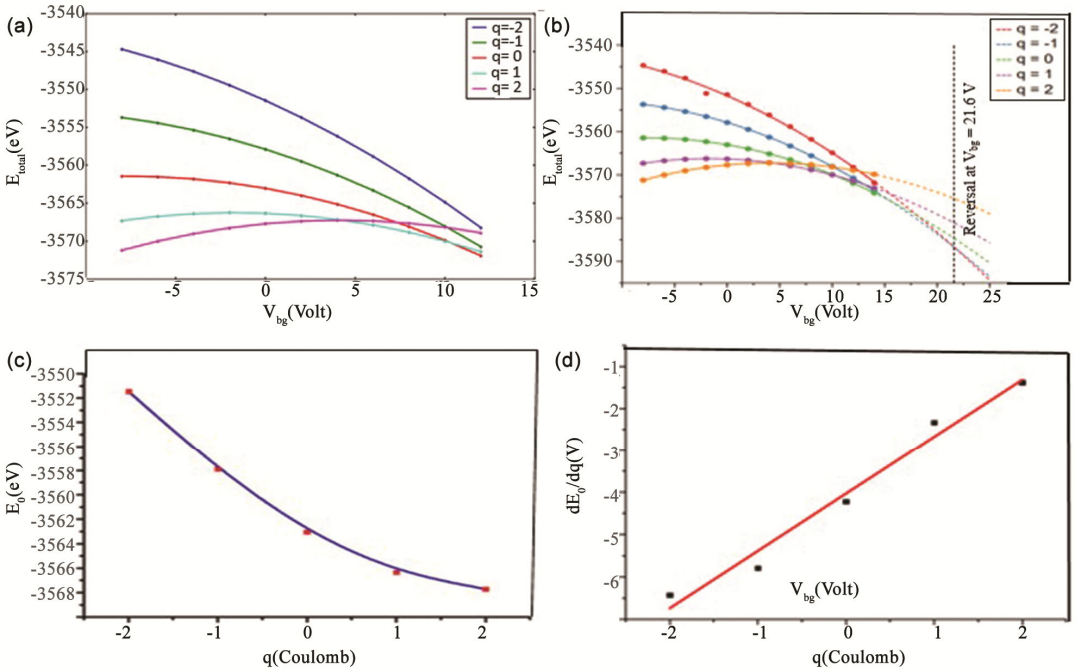

Fig. 3 — Plot of (a) E_{total}versus V_{bg} for the TG- SET for different charge states $q = -2\ to\ +2$, (b) E_{total}versus V_{bg} extrapolated to $V_{bg} = 25\,V$. (Dotted lines represent extrapolated polynomial fits and circular dots denote simulated data. A reversal in energy ordering occurs at V_{bg}~21.6 V, where all charge states invert their energy sequence), (c) E_0 versus q at $V_{bg} = 0$, and (d) $\frac{dE_0}{dq}$ versus q

Table 1 — Ionization, affinity and addition energy for single, double and triple gated SETs #

Energy Parameter	SG-SET[18] (eV)	DG-SET [18](eV)	TG-SET (eV)
Second ionization	7.86	5.13	3.90
First ionization	5.50	3.15	1.99
First affinity	3.08	1.26	0.12
Second affinity	0.34	0.05	1.15
Addition energy	2.42	1.89	1.87

To better comprehend how the extra gate in the TG-SET impacts, voltages of top gate (V_{tg}) and back gate (V_{bgv}) were fixed at a value of $-8\,V$. The connection between bottom gate voltage (V_{bg}), and total energy (E_{total}), is illustrated in Fig. 3(a). It is visible from Fig. 3(a) that the minimum energy of neutral molecule is attained at $V_{bg} = 12\,V$ in TG-SET compared to $V_{bg} = 10\,V$ in case of DG-SET, at fixed top gate voltage $V_{bgv} = -8\,V$. In order to explore the behaviour of E_{total} with V_{bg}, beyond the simulated range of 14 V, we fitted the simulated data into the following expression.

$$E_{total} = \alpha q V_{bg} + (\beta e V_{bg})^2, \qquad \ldots (1)$$

where α (gate coupling constant) is the coefficient depicting the linear dependence of E_{total} on qV_{bg} and β is the coefficient depicting the quadratic dependence. This fitted data was further extrapolated to the range 14 V ≤ V_{bg} ≤ 25 V as shown in Fig. 3(b). Figures 3(c –d) depict behaviour of E_0 (E $_{Total}$ at V$_{bg}$=0) versus q and the derivative of E_0 with respect to q versus q respectively.

Figure 3(b) depicts the E_{total} variation as a function of V_{bg} for charge states $q = -2$ to $+2$. The simulated data points are shown along with the quadratic polynomial fits across the full voltage range (i.e. simulated V_{bg} up to 14 V and extrapolated V_{bg} up to 25 V. At lower gate voltages, the total energy trend exhibits a monotonic increase in energy with decreasing charge, with the $q = -2$ state having the highest energy and q = +2 the lowest energy. This is attributed to the dominant Coulomb repulsion in more negatively charged configurations. However, as V_{bg} increases, the negative charge states ($q = -2\ and\ q = -1$) exhibit sharper energy declines, while the positive states decrease gradually. This differential response results in a complete reordering of energy levels at higher voltages. The crossover point, where the energy

sequence $E_{total}(q)$ becomes $E_{total}(-2) < E_{total}(-1) < E_{total}(0) < E_{total}(+1) < E_{total}(+2)$, occurs at approximately V_{bg}~$21.6\,V$. These extrapolations not only reinforce the gate-tunable nature of the TG-SET but also help estimate addition energies with greater accuracy when direct simulations are limited by computational constraints. Such gate-induced modulation is critical for enabling precise control over charge states in molecular-scale devices and demonstrates the suitability of the tri-gated architecture for advanced charge-based switching and sensing applications.

Further a positive bottom gate voltage, V_{bg}, enables the molecule to acquire an extra electron, resulting in a molecule with a positive charge as the LUMO level moves closer to the Fermi level of electrode. Conversely, as the HUMO level rises approaching the electrode's Fermi level, a negative V_{bg} permits the molecule to lose one electron, resulting in a positively charged state as well.

In Eq. (1), the linear term $\alpha q V_{bg}$, suggests a strong connection to the bottom gate and the quadratic term $(\beta e V_{bg})^2$ is attributed to the polarization of the island and does not depend on q.[29] The value of the gate coupling constant, α is determined to be 0.5168 for the TG- SET, which is better than the α value of 0.3502 for the DG- SET and 0.4898 for the single-gated SET.

The relationship between total energy at zero bottom gate voltage (E_0) and the charge state q is illustrated in Fig. 3(c). It shows that as the q values increase, the E_0 values decrease. For negative q values, when V_{bgv} and V_{tg} are less than zero, it is more energetically expensive to extract an electron out of the molecule, compared to the case when q has positive values. Fig. 3(d) depicts the derivative of E_0 with respect to q, the curve that results is linear, showing that the energy shift brought about by adding or subtracting a charge from the molecule at a particular q state is directed in the opposite direction. The slope of this line is determined to be 1.356.

In Fig. 4, the charge stability diagrams (CSDs) are presented for the TG- SET to explore the conduction behaviour and E_{total} in relation to V_{bg}. Figure 4(a - b) correspond to V_{tg} and V_{bgv} values of -8 V, with Fig. 4(b) providing a closer view of a section from Fig. 4(a). Electron transport between the source and drain is observed in weak coupling regime only when the energy levels of a molecule fall within the bias window defined by the applied bias between source and drain V_d. The diamonds in the CSD indicate the accessible conductive regions that separate conductive from non-conductive areas for

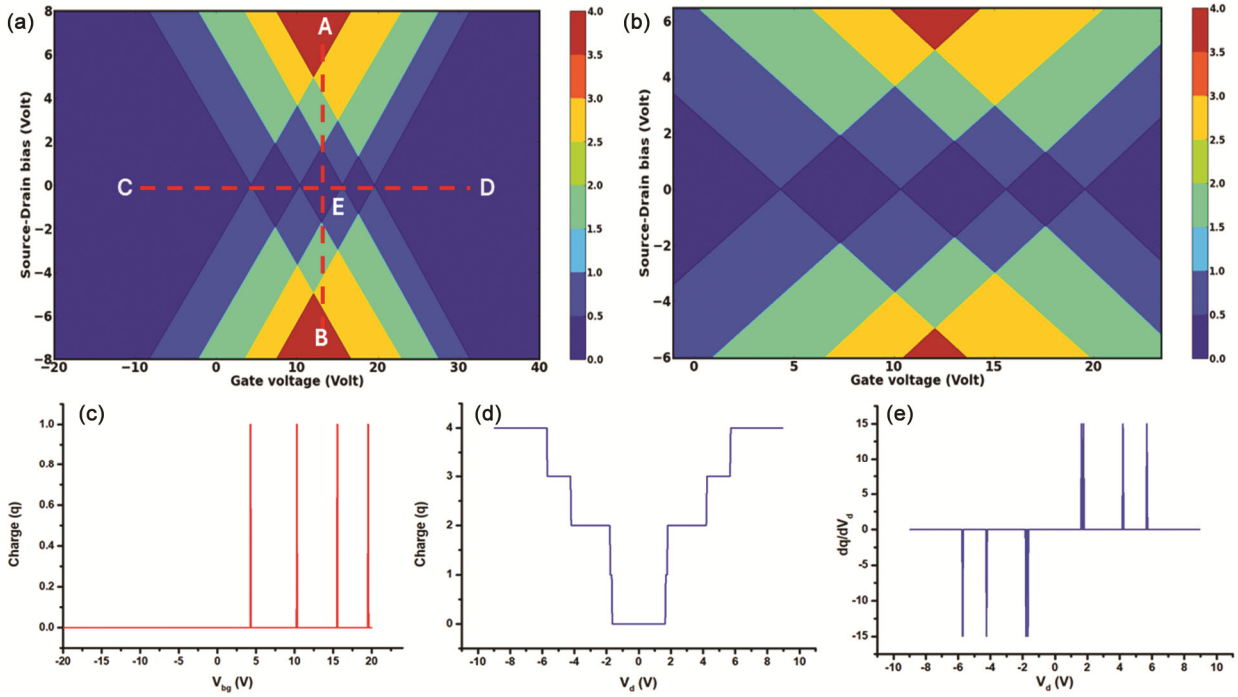

Fig. 4 — Charge stability diagram (CSD) (a) for tri-gated SET at $V_g = -8\,V$, (b) central diamond part of the CSD (zoomed), (c) tracing along C-D, (d) tracing along A-B, (e) differential charge $\frac{dq}{dV_d}$ as a function of V_d

various V_{bg} and V_d values. Each diamond's color represents different conductive zones, conduction can be seen ascending in the sequence of dark blue, light blue, green, yellow, and red. Figure 4(a) shows the key conduction region, marked by A, B, C, and D. It highlights the successive tunneling between various charge states within the central diamond area. The magnified section shown in Fig. 4(b) illustrates the ground state excitation behaviour of molecules. The central diamond, which hypothetically contains m electrons, signifies the molecule's neutral charge state in its ground state. The electron population on the molecule remains constant inside the diamonds, only changing while moving from one to another.

It is possible to estimate the charging energy of the ground state as the central diamond's height, which is $3.428\,eV$. For the anionic molecular state (the state with $m + 1$ electrons), the right diamond's height is $2.606\,eV$, whereas the left diamond's height is $3.846\,eV$, which corresponds to the cationic molecular state (the state with $m - 1$ electrons). Compared to the DG-SET, which has charging energy of $3.440\,eV$ for ground state and right and left diamond heights of $2.696\,eV$ and $4.04\,eV$, respectively, these figures are comparatively lower. Therefore, the TG-SET exhibits greater conductivity compared to the double-gated SET. To estimate the energy E_{add} i.e. the energy needed to produce the cationic and anionic states of the molecule, we have used the following expression.

$$E_{add} = (E_{m-1} - E_m) - (E_m - E_{m+1})$$
$$\text{i.e. } E_{add} = E_{m+1} + E_{m-1} - 2E_m \quad ...(2)$$

where m represents the specific number of electrons present in the molecule's neutral state. The TG-SET's observed addition energy is $1.86\,eV$, which is less than the DG-SET's $1.89\,eV$ and less than that of the single-gate SET at $2.42\,eV$. Thus, it is possible to obtain comprehensive electrostatic details of the SET from the CSD curve.

The lines C–D and A–B are traced horizontally and vertically, respectively, in Figs 4(c-d). As V_{bg} increases from left to right, sharp peaks can be seen, indicating the change in the conduction window as the molecule either accepts or rejects an individual electron. All of the peaks have a maximum charge value of 1, as the sole transition from the ground state to the first excited state takes place at low values of source drain voltage V_d. In the vertical trace, symmetric periodic plateaus appear on either side of the $V_d = 0$. The steps pattern seen for finite levels of charge q demonstrates the absence of continuous transport. The plateau's breadth indicates that the charging energy is $3.28\,eV$ at a fixed $V_{bg} = 13.18\,V$, which is lower than the value of $3.392\,eV$ observed in a double-gate SET. The differential charge plot dq/dV_d, presented in Fig. 4(e), provides a detailed understanding of the staircase plateaux, which, during the discontinuous transit at a low tunneling rate, indicate charging to the excited state at particular V_d values. The spacing between successive excited states indicates the charging energy of a molecule at a fixed $V_{bg} = 0.008\,V$.

4 Conclusion

Computational studies of a triple-gated single-electron transistor (SET) have been conducted using vanadium tris(dithiolene) [V(edt)$_3$] (where edt refers to 1,2-ethenedithiolate) as the island molecule. The TG-SET demonstrates significantly enhanced performance and substantially improved electrostatic control when compared to both double-gate and single-gate SETs. To gain a deeper understanding of the conduction characteristics, the calculated molecular energy is used to plot CSDs at various gate voltages. Successive tunneling of electrons and their non-continuous passage through the system are shown by the CSDs' vertical and horizontal traces. The energy levels of a molecule are very responsive to various gate voltages, which vary significantly with different charge states, hence these SETs can function as rapid and portable charge sensors for next generation nanoelectronic gadgets.

Due to computational constraints posed by extended voltage ranges, extrapolation techniques within a carefully considered range had to be used beyond $V_{bg} = 14\,V$ to estimate the energy re-ordering behaviour. It is found that total energy versus q state values get reordered after $V_{bg} = 21.6\,V$ at the bottom gate, a useful feature for fine tuning the TG-SET architecture with charge state in various switching and sensing applications.

Though, in this work, we have focused on the V(edt)$_3$ molecule due to its excellent redox behaviour and structural stability, evaluating other molecular systems in future could further validate and expand the TG-SET concept. Further the simulations, based on static DFT and NEGF frameworks, effectively capture key electrostatic and transport features, future work, however, may incorporate time-dependent DFT

(TD-DFT) and ab initio molecular dynamics (AIMD) to capture transient and thermally driven effects. Experimental synthesis and electrical characterization of TG-SETs are also critical next steps to confirm theoretical predictions and address practical fabrication challenges such as gate alignment, leakage minimization, and integration into CMOS-compatible platforms. Thus, incorporating time-dependent simulations, molecular dynamics, and experimental testing will help bridge the gap between theory and practical device realization, particularly in CMOS-compatible platforms.

Acknowledgements

The authors acknowledge the contribution of the Indian Institute of Information Technology and Management (ABV), Gwalior, Madhya Pradesh, and Jamia Millia Islamia, New Delhi, India, for providing the computing resources needed to conduct the study and Acharya Narendra Dev College, University of Delhi, Delhi, India for the institutional support.

References

1 Das K, Lehmann T & Dzurak A S, *IEEE Trans Circuits Syst I Regul Pap*, 61(10) (2014) 2816.
2 Villis B J, Orlov A O, Barraud S, Vinet M, Sanquer M, Fay P, Snider G & Jehl X, *Appl Phys Lett*, 104(23) (2014) 233503.
3 Schoelkopf R J, Wahlgren P, Kozhevnikov A A, Delsing P & Prober D E, *Science*, 280(5367) (1998) 1238.
4 Berman D, Zhitenev N B, Ashoori R C, Smith H I & Melloch M R, *J Vac Sci Technol B*, 15(6) (1997) 2844.
5 Srivastava A, Santhibhusha B & Dobwal P, *Int J Nanosci*, 12(06) (2013) 1350045.
6 Srivastava A, Santhibhushan B & Dobwal P, *Appl Nanosci*, 4 (2014) 263.
7 Ray S J, *J Appl Phys*, 116(24) (2014) 034307.
8 Kaasbjerg K & Flensberg K, *Nano Lett*, 8(11) (2008) 3809.
9 Matsumoto K, Ishii M, Segawa K, Oka Y, Vartanian B J & Harris J S, *Appl Phys Lett*, 68(1) (1996) 34.
10 Fulton T A & Dolan G J, *Phys Rev Lett*, 59(1) (1987) 109.
11 Anu, Sharma A, Khan M S, Srivastava A, Husain M & Khan M S, *IEEE Trans Electron Devices*, 64(11) (2017) 4628.
12 Anu, Srivastava A & Khan M S, *Org Electron*, 53 (2018) 227.
13 Xu H, Chen R, Sun Q, Lai W, Su Q, Huang W & Liu X, *Chem Soc Rev*, 43(10) (2014) 3259.
14 Kalyanasundaram K & Grätzel M, *Coord Chem Rev*, 177(1) (1998) 347.
15 Zhao J H, Hu Y X, Lu H Y, Lü Y L & Li X, *Org Electron*, 41 (2017) 56.
16 Duprez V, Biancardo M & Krebs F C, *Sol Energy Mater Sol Cells*, 91(4) (2007) 230.
17 Xiaohui L, Qingqing W, Jie B, Songjun H, Wenlin J, Chun-Liang T, Hang S, Xiaojuan H, Jueting Z, Yang Y, Junyang L, Yong H, Jia S, Zitong L, Lambert C, Deqing Z & Wenjing H, *Angew Chem Int Ed*, 59(8) (2020) 3280.
18 Anu, Srivastava A & Khan M S, *J Electron Mater*, 49 (2020) 4203.
19 Ray S J, *J Appl Phys*, 119(20) (2016) 204302.
20 Frisch M J, Trucks G W, Schlegel H B, Scuseria G E, Robb M A, Cheeseman J R, Montgomery J A, Vreven T, Kudin K N, Burant J C & Millam J M, *GAUSSIAN 03*, Gaussian Inc. (Wallingford), 2004.
21 Stokbro K, *J Phys Chem C*, 114(48) (2010) 20461.
22 Kaasbjerg K & Flensberg K, *Nano Lett*, 8(11) (2008) 3809.
23 Riviere J C, *Appl Phys Lett*, 8(7) (1966) 172.
24 Brandbyge M, Mozos J L, Ordejón P, Taylor J & Stokbro K, *Phys Rev B*, 65(16) (2002) 165401.
25 Smidstrup S, Markussen T, Vancraeyveld P, Wellendorff J, Schneider J, Gunst T, Verstichel B, Stradi D, Khomyakov P A, Vej-Hansen U G & Lee M E, *J Phys Condens Matter*, 32(1) (2019) 015901.
26 Mitsuru K K, Seika M, Kazuko I, Hiroyuki M, Nobumasa K & Susumu K, *Chem Lett*, 25 (1996) 489.
27 Srivastava A, Santhibhushan B, Sharma V, Kaur K, Shahzad Khan M, Marathe M, De Sarkar A & Shahid Khan M, *J Electron Mater*, 45 (2016) 2233.
28 Shityakov S, Roewer N, Förster C & Broscheit J A, *Nanoscale Res Lett*, 12 (2017) 1.
29 Srivastava A, Kaur K, Sharma R, Chauhan P, Sharma U S & Pathak C, *J Electron Mater*, 43 (2014) 3449.